

An Outline of the Structure of New Layered Bismuth Lanthanum Tungstate, $\text{Bi}_{2-x}\text{La}_x\text{WO}_6$ ($x = 0.4-1.1$)

A. WATANABE, Y. SEKIKAWA, AND F. IZUMI

National Institute for Research in Inorganic Materials, 1-1 Namiki, Sakura-mura, Niihari-gun, Ibaraki 305 Japan

Received August 26, 1981

An outline of the structure of a continuous solid-solution series $\text{Bi}_{2-x}\text{La}_x\text{WO}_6$ with $x = 0.4-1.1$ (space group $P2/c$ and $Z = 8$) has been determined from a lattice imaging method of electron microscopy. A high-resolution lattice image of $\text{Bi}_{1.4}\text{La}_{0.6}\text{WO}_6$ selected as representative of the series showed that the structure consists of a regular stacking of $\text{Bi}_{1.4}\text{La}_{0.6}\text{O}_2$ layers interleaved with WO_4 layers. A structural model of $\text{Bi}_{2-x}\text{La}_x\text{WO}_6$ was proposed and atomic coordinates were estimated on the basis of the model. The structural relations between $\text{Bi}_{2-x}\text{La}_x\text{WO}_6$ and Bi_2WO_6 were discussed.

Introduction

A new continuous solid-solution series with composition $\text{Bi}_{2-x}\text{La}_x\text{WO}_6$ has been found over a limited range of x between 0.4 and 1.1 at 1050°C (1, 2). The single crystal X-ray diffraction patterns showed that the series has monoclinic $P2/c$ symmetry all over the range; although $P2/a$ was assigned in the previous papers (1-3), another monoclinic setting $P2/c$ is selected here in order to contrast the structure of the series with that of Bi_2WO_6 (space group $B2cb$ with $a = 5.457$, $b = 5.436$, $c = 16.427$ Å, and $Z = 4$) (4). The unit cell of $\text{Bi}_{2-x}\text{La}_x\text{WO}_6$ contained eight formula-units and Raman spectra indicated that its structure included WO_4 tetrahedra with no oxygens in common (1). Moreover the platelike morphology of the grown $\text{Bi}_{1.4}\text{La}_{0.6}\text{WO}_6$ single crystals suggested that this series has a layered structure (1). As seen from the chemical formula $\text{Bi}_{2-x}\text{La}_x\text{WO}_6$, this solid-solution series was prepared by substituting La^{3+} for part of Bi^{3+} in Bi_2WO_6 which is the simplest

member of the bismuth oxide layer structure family (5); the structure of Bi_2WO_6 consists of Bi_2O_2 layers comprising BiO_4 pyramids sandwiched between WO_4 layers containing corner-linked WO_6 octahedra as shown in Fig. 2b. On one hand, the La^{3+} ions also show a preference for pyramidal coordination in the layer-type compound La_2MoO_6 (6) to form La_2O_2 layers similar to the Bi_2O_2 layers. Therefore, from the point of view of a structural correlation of this series with Bi_2WO_6 and from Raman spectra, it is deduced that the structure of $\text{Bi}_{2-x}\text{La}_x\text{WO}_6$ is comprised of a regular stacking of $\text{Bi}_{2-x}\text{La}_x\text{O}_2$ layers interleaved with WO_4 layers containing isolated WO_4 tetrahedra. This suggestion induced us to study the crystal structure for $\text{Bi}_{2-x}\text{La}_x\text{WO}_6$ by super-high-resolution electron microscopy. Samples with composition $\text{Bi}_{1.4}\text{La}_{0.6}\text{WO}_6$ were employed here as representative of the system; lattice parameters of this compound are as follows: $a = 8.280$, $b = 7.683$, $c = 16.407$ Å and $\beta = 102.18^\circ$ (1).

Experimental

Single crystals with composition $\text{Bi}_{1.4}\text{La}_{0.6}\text{WO}_6$ were grown in the same way as previously described (1).

A high-voltage electron microscope, Hitachi-1250kV Type, was used to observe high-resolution lattice images. The platelike single crystals were finely crushed in an agate mortar to yield fragments a few microns in size and then the finer fragments were set on a carbon mesh supporting film. Details of the instrumentation and operation of the microscope were reported elsewhere (7, 8).

An X-ray powder diffraction pattern was taken using a conventional diffractometer with Ni-filtered $\text{CuK}\alpha$ radiation. The rela-

tive intensity of possible Bragg reflections was calculated and the results were represented as a corresponding powder pattern (Fig. 3).

Results and Discussion

Figure 1 exhibits a lattice image taken with the incident beam parallel to the projection axis [010]. A corresponding electron diffraction pattern is attached for reference. The results obtained from this diffraction pattern agreed well with those based on the X-ray measurements: the aforementioned lattice parameters (a , c , and β) and the systematic absence ($l = 2n + 1$ for both $h0l$ and $00l$) due to $P2/c$ symmetry. As ex-

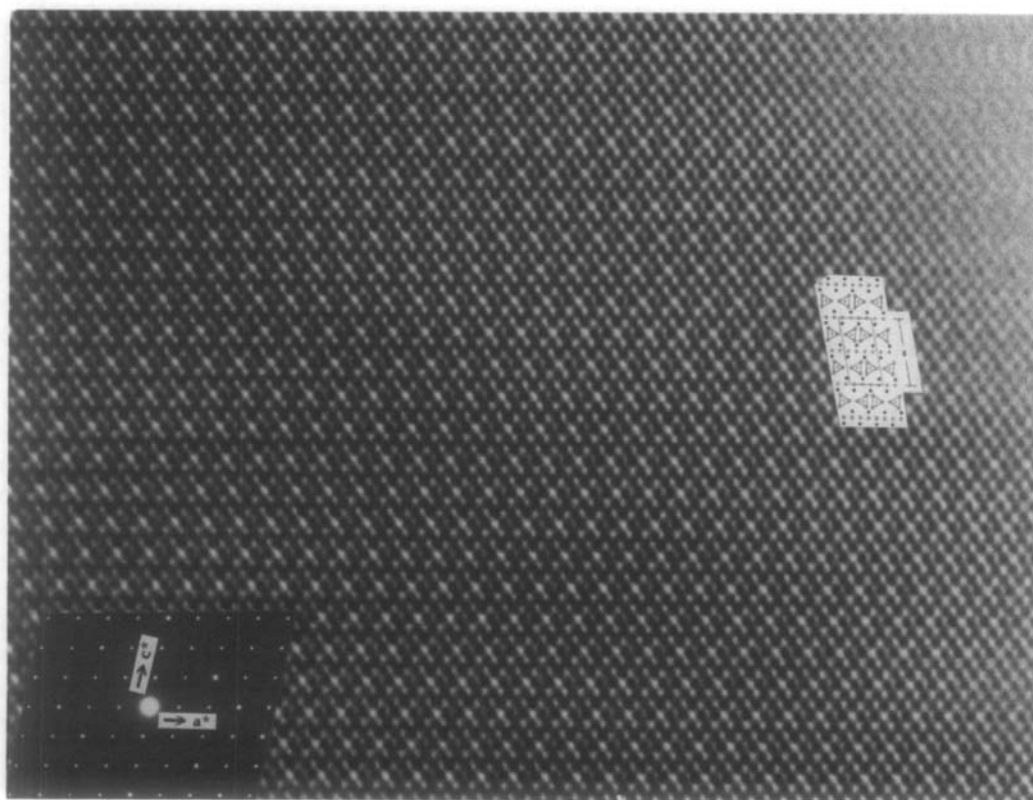


FIG. 1. A lattice image of $\text{Bi}_{1.4}\text{La}_{0.6}\text{WO}_6$ projected on (010). Insets: a corresponding electron diffraction pattern and a proposed structure model. Large solid circles denote Bi or La, small solid circles W and open circles O. The length $c = 16.4 \text{ \AA}$.

pected, the lattice image shows two types of layers which appear alternately in parallel with dark spots of contrast: zigzag spots at the positions of $\text{Bi}_{1.4}\text{La}_{0.6}\text{O}_2$ layers and one-dimensional periodic arrays of a pair of spots at WO_4 layers, which consist of isolated WO_4 tetrahedra according to Raman spectra (1). Consequently the zigzag spots correspond to Bi or La atoms and the remaining rows of a pair of spots to W atoms. In the $\text{Bi}_{1.4}\text{La}_{0.6}\text{O}_2$ layers, Bi and La atoms are randomly distributed in the apex sites of pyramidal configuration, because reflections caused by a superstructure were not able to be observed in both X-ray and electron diffraction patterns. Thus the lattice image and $P2/c$ symmetry of $\text{Bi}_{1.4}\text{La}_{0.6}\text{WO}_6$ led to a structural model inserted in Fig. 1. At the same time, an outline of the unit cell of the proposed $\text{Bi}_{2-x}\text{La}_x\text{WO}_6$ structure is illustrated in Fig. 2 together with the structure of Bi_2WO_6 projected on (110) for comparison. As for the WO_4 layers, atomic coordinates for the oxygen atoms surrounding tungsten atoms were roughly estimated by analogy with the scheelite (CaWO_4) structure (9, 10); in fact, the senses of the tetrahedra cannot be determined from the $P2/c$ symmetry alone.

The space group $P2/c$ contains seven

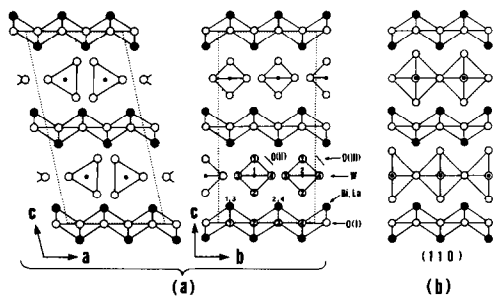


FIG. 2. Schematic representation of crystal structures: (a) a proposed crystal structure of $\text{Bi}_{2-x}\text{La}_x\text{WO}_6$ ($x = 0.4-1.1$) projected on (010) and (100); (b) the idealized structure of Bi_2WO_6 projected on (110). Large hatched circles denote Bi or La in (a) and Bi in (b); the other symbols are the same as in Fig. 1.

TABLE I
ESTIMATED POSITIONAL PARAMETERS FOR
 $\text{Bi}_{2-x}\text{La}_x\text{WO}_6$ ($x = 0.4-1.1$) WITH SPACE GROUP
 $P2/c$ AND $Z = 8^a$

Atom	x	y	z
$(\text{Bi}_{2-x}\text{La}_x)(1)$	0.902	0.125	0.0653
(2)	0.902	0.625	0.0653
(3)	0.402	0.125	0.0653
(4)	0.402	0.625	0.0653
W(1)	0.296	0.375	0.250
(2)	0.296	0.875	0.250
O(I)(1)	0.125	0.125	0.000
(2)	0.375	0.375	0.000
(3)	0.125	0.625	0.000
(4)	0.375	0.875	0.000
O(II)(1)	0.459	0.375	0.341
(2)	0.383	0.375	0.159
(3)	0.171	0.185	0.250
(4)	0.171	0.565	0.250
O(III)(1)	0.459	0.875	0.341
(2)	0.383	0.875	0.159
(3)	0.171	0.684	0.250
(4)	0.171	0.065	0.250

^a Atomic coordinates: general position $4g$ (x, y, z), ($\bar{x}, \bar{y}, \bar{z}$), ($\bar{x}, y, \frac{1}{2} - z$), ($x, \bar{y}, \frac{1}{2} + z$).

equipoints: one general and six special sites. General position $4g$ consists of (x, y, z), ($\bar{x}, \bar{y}, \bar{z}$), ($\bar{x}, y, \frac{1}{2} - z$) and ($x, \bar{y}, \frac{1}{2} + z$). Special positions are as follows: $2a$ ($0, 0, 0$), ($0, 0, \frac{1}{2}$); $2b$ ($\frac{1}{2}, \frac{1}{2}, 0$), ($\frac{1}{2}, \frac{1}{2}, \frac{1}{2}$); $2c$ ($0, \frac{1}{2}, 0$), ($0, \frac{1}{2}, \frac{1}{2}$); $2d$ ($\frac{1}{2}, 0, 0$), ($\frac{1}{2}, 0, \frac{1}{2}$); $2e$ ($0, y, \frac{1}{4}$), ($0, \bar{y}, \frac{3}{4}$); $2f$ ($\frac{1}{2}, y, \frac{1}{4}$), ($\frac{1}{2}, \bar{y}, \frac{3}{4}$). As is evident from the atomic positions depicted in Fig. 2a, however, no atom occupies the special positions; therefore, all atoms were assigned to the general positions. Thus approximate atomic coordinates for $\text{Bi}_{2-x}\text{La}_x\text{WO}_6$ were obtained from this model. Table I lists the positional parameters estimated, where oxygens O(I) are included in the $\text{Bi}_{2-x}\text{La}_x\text{O}_2$ layers, while O(II) and O(III) surround W to form the WO_4 layers.

As a check on the correctness of the structure proposed, the relative intensity based on the model was calculated for $\text{Bi}_{1.4}\text{La}_{0.6}\text{WO}_6$. The result is shown in Fig. 3

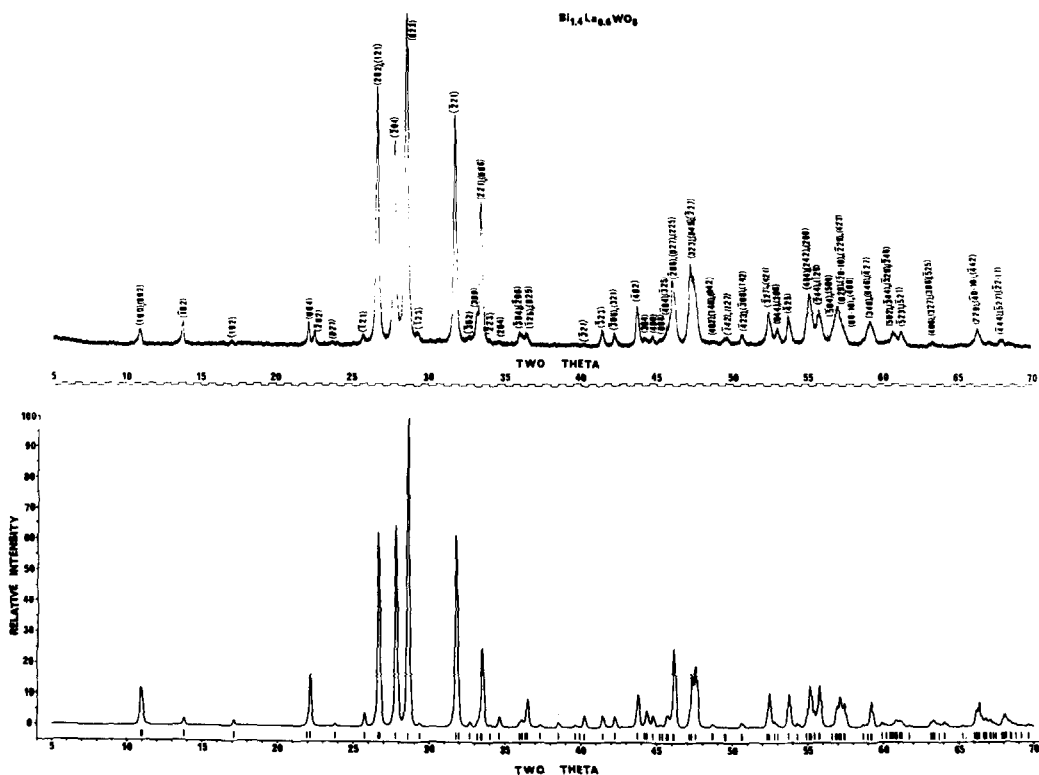


FIG. 3. The observed and calculated powder diffraction patterns for $\text{Bi}_{1.4}\text{La}_{0.6}\text{WO}_6$ (space group $P2/c$ with $a = 8.280$, $b = 7.683$, $c = 16.407$ Å, $\beta = 102.18^\circ$, and $Z = 8$). The upper curve is the observed pattern which was measured by Ni-filtered $\text{CuK}\alpha$ (30 kV/10 mA) radiation. The lower curve means the calculated one; the short vertical lines indicate the positions of possible Bragg reflections with the calculated relative intensity above 1%.

along with the observed X-ray powder pattern. On comparing the two curves, it is clear that the parameters for $\text{Bi}_{2-x}\text{La}_x\text{WO}_6$ given in Table I are fairly good approximations except for those of O(II) and O(III). Using these approximate values, the structure should be refined with single-crystal X-ray diffraction or neutron diffraction analysis; in particular, the latter method is useful to ascertain the oxygen positions.

As contrasted with the structure of Bi_2WO_6 shown in Fig. 2b, the series $\text{Bi}_{2-x}\text{La}_x\text{WO}_6$ has also layered structure and the main orientation relations are found to be $[100]_{\text{BLW}}//[110]_{\text{BW}}$ and $[010]_{\text{BLW}}//[1\bar{1}0]_{\text{BW}}$ (where subscripts BLW and BW denote $\text{Bi}_{2-x}\text{La}_x\text{WO}_6$ and Bi_2WO_6 ,

respectively). Accordingly, the unit cell of $\text{Bi}_{2-x}\text{La}_x\text{WO}_6$ is approximately related to that of Bi_2WO_6 as follows: $a_{\text{BLW}} \approx b_{\text{BLW}} \approx \sqrt{2}(a_{\text{BW}} + b_{\text{BW}})/2$; $c_{\text{BLW}} \approx c_{\text{BW}}$. However, as seen from Fig. 2, Bi_2WO_6 has W in 6-coordination; $\text{Bi}_{2-x}\text{La}_x\text{WO}_6$ is quite different, with 4-coordinated W. The difference in the tungsten coordination appears to depend on the degree of the $6s^2$ lone-pair character of Bi^{3+} . That is, in Bi_2WO_6 the lone-pair character is dominant, so that each Bi^{3+} forms the fifth pair bond with an oxygen of the WO_4 layer consists of corner-linked WO_6 octahedra. On the other hand, in $\text{Bi}_{2-x}\text{La}_x\text{WO}_6$ the lone-pair character is constrained because of the interaction between Bi^{3+} and La^{3+} (J); therefore, the

bond does not exist between the $\text{Bi}_{2-x}\text{La}_x\text{O}_2$ layer and the WO_4 layer, and isolated WO_4 tetrahedra are eventually formed in the latter layer.

A series of compounds BiLnWO_6 have been synthesized for all Ln^{3+} (Ln = rare earth, including La and Y) and solid-solution series $\text{Bi}_{2-x}\text{Ln}_x\text{WO}_6$ have also been prepared for some typical Ln^{3+} s (2). They had a monoclinic $P2/c$ structure similar to that of $\text{Bi}_{2-x}\text{La}_x\text{WO}_6$; hence, all of them would presumably seem to be isomorphous. Namely, they have structures with alternating $\text{Bi}_{2-x}\text{Ln}_x\text{O}_2$ and WO_4 layers.

The cell volumes of the $\text{Bi}_{2-x}\text{Ln}_x\text{WO}_6$ series varied linearly with Ln concentration x , and the slopes of the straight lines depended on the ionic radii of Ln^{3+} s; furthermore, in these plots, all extrapolation lines to $x = 0.0$ converged to give a cell volume corresponding to hypothetical monoclinic Bi_2WO_6 (2). This suggested the presence of a modification of Bi_2WO_6 . In fact, the actual orthorhombic Bi_2WO_6 undergoes a reversible polymorphic transformation at about 960°C on heating, accompanied by a remarkable volume expansion. High-temperature powder X-ray diffraction measurements were made for Bi_2WO_6 with a view to identifying a high-temperature stable form of it (12). Results showed that the high-temperature form had a monoclinic symmetry which may be isomorphous with the $\text{Bi}_{2-x}\text{La}_x\text{WO}_6$ series. To sum up, in Bi_2WO_6 the lone-pair character of Bi^{3+} seems to be constrained by thermal energies above the transformation temperature to form the monoclinic high-temperature modification

as well as by partial replacement of Bi^{3+} by Ln^{3+} over a limited range of x to form the monoclinic solid-solution $\text{Bi}_{2-x}\text{Ln}_x\text{WO}_6$ series.

In conclusion, the lattice imaging method is extremely useful to investigate crystal structures. In particular, high-resolution lattice images taken with a high-voltage electron microscope give helpful information upon the structural outline. At present, however, atomic positions for oxygens cannot be determined directly by this method, so that the refinement of the structure of $\text{Bi}_{2-x}\text{La}_x\text{WO}_6$ must be left for a future study.

References

1. A. WATANABE, Z. INOUE, AND T. OHSAKA, *Mat. Res. Bull.* **15**, 397 (1980).
2. A. WATANABE, *Mat. Res. Bull.* **15**, 1473 (1980).
3. Z. INOUE AND A. WATANABE, *J. Mat. Sci.* **15**, 2669 (1980).
4. R. W. WOLFE, R. E. NEWNHAM, AND M. I. KAY, *Solid State Comm.* **7**, 1797 (1969).
5. E. C. SUBBARAO, *J. Phys. Chem. Solids* **23**, 665 (1962).
6. L. G. SILLÉN AND K. LUNDBORG, *Z. Anorg. Chem.* **252**, 2 (1943).
7. Y. BANDO, A. WATANABE, Y. SEKIKAWA, M. GOTO, AND S. HORIUCHI, *Acta Crystallogr. Sect. A* **35**, 142 (1979).
8. S. HORIUCHI, Y. MATSUI, Y. BANDO, T. KATSUTA, AND I. MATSUI, *J. Electron Microsc.* **27**, 39 (1978).
9. A. ZALKIN AND D. H. TEMPLETON, *J. Chem. Phys.* **40**, 501 (1964).
10. M. I. KAY, B. C. FRAZER, AND I. ALMODOVAR, *J. Chem. Phys.* **40**, 504 (1964).
11. R. E. NEWNHAM, R. W. WOLFE, AND J. F. DORRIAN, *Mat. Res. Bull.* **6**, 1029 (1971).
12. A. WATANABE, *J. Solid State Chem.* **41**, 160 (1982).